JOURNAL OF GEOPHYSICAL RESEARCH, VOL. 110, B09409, doi:10.1029/2004JB003556, 2005

Surface mass redistribution inversion from global GPS deformation and Gravity Recovery and Climate Experiment (GRACE) gravity data

J. Kusche and E. J. O. Schrama

Delft Institute of Earth Observation and Space Systems, Delft University of Technology, Delft, Netherlands

Received 29 November 2004; revised 15 April 2005; accepted 17 May 2005; published 20 September 2005.

[1] Monitoring hydrological redistributions through their integrated gravitational effect is the primary aim of the Gravity Recovery and Climate Experiment (GRACE) mission. Time-variable gravity data from GRACE can be uniquely inverted to hydrology, since mass transfers located at or near the Earth's surface are much larger on shorter timescales than those taking place within the deeper Earth and because one can remove the contribution of atmospheric masses from air pressure data. Yet it has been proposed that at larger scales this may be achieved independently by measuring and inverting the elastic loading associated with redistributing masses, e.g., with the global network of the International GPS Service (IGS). This is particularly interesting as long as GRACE monthly gravity solutions do not (yet) match the targeted baseline accuracies at the lower spherical harmonic degrees. In this contribution (1) we describe and investigate an inversion technique which can deal jointly with GPS data and monthly GRACE solutions. (2) Previous studies with GPS data have used least squares estimators and impose solution constraints through low-degree spherical harmonic series truncation. Here we introduce a physically motivated regularization method that guarantees a stable inversion up to higher degrees, while seeking to avoid spatial aliasing. (3) We apply this technique to GPS data provided by the IGS service covering recent years. We can show that after removing the contribution ascribed to atmospheric pressure loading, estimated annual variations of continental-scale mass redistribution exhibit pattern similar to those observed with GRACE and predicted by a global hydrology model, although systematic differences appear to be present. (4) We compute what the relative contribution of GRACE and GPS would be in a joint inversion: Using current error estimates, GPS could contribute with up to 60% to degree 2 till 4 spherical harmonic coefficients and up to 30% for higher-degree coefficients.

Citation: Kusche, J., and E. J. O. Schrama (2005), Surface mass redistribution inversion from global GPS deformation and Gravity Recovery and Climate Experiment (GRACE) gravity data, *J. Geophys. Res.*, *110*, B09409, doi:10.1029/2004JB003556.

1. Introduction

[2] The primary objective of the GRACE mission is to monitor hydrological mass redistributions through their integrated gravitational effect [*Tapley et al.*, 2004]. In August 2004, the first monthly gravity fields have been released to the public, covering April 2002 to April 2004. Yet it has been proposed by *Blewitt et al.* [2001] and *Blewitt and Clarke* [2003] that at larger scales this may be achieved independently by geometrically measuring the elastic response of the Earth to the loading associated with redistributing masses, e.g., with the global network of the International GPS Service. This is particularly interesting as long as GRACE monthly gravity solutions do not (yet) match the targeted baseline accuracy at the lower degrees.

[3] In principle, gravity field changes sensed by the two GRACE satellites and surface loading observed by GPS networks include the combined direct and indirect effect of all mass redistributions within the Earth and its atmospheric and fluid envelope. It is well know that one cannot uniquely solve for 3D density distributions from gravity data; however, the majority of the mass transports important on timescales from daily to interannual occur at or near the Earth's surface [*Chao*, 2005]. Under this hypothesis, gravity changes on these timescales can be uniquely inverted into mass redistribution within a spherical shell at the surface. Because the atmospheric contribution to the surface density change can be reasonably modeled using atmospheric pressure data, GRACE gravity and GPS displacements allow to detect changes in the Earth's larger hydrological storage systems.

[4] However, in any case, the analyst is forced to constrain solved-for mass configurations either by low-degree truncation, by spatial averaging [*Swenson and Wahr*, 2002],

0148-0227/05/2004JB003556$09.00

or by regularization operations employing mathematically or physically motivated constraints. This is because the errors in GRACE or GPS-derived spherical harmonic coefficients are not "white" over the spectral domain but increase with higher resolution because load Love numbers quickly lose their power and so the spectral sensitivity decreases, and in the case of GPS inversion, the Earth's coverage with observations is far from homogeneous. Combining satellite gravity and geometrical displacements in a joint inversion may help to relieve these constraints and improve the reliability of estimates, but in particular, it offers prospects for cross validation and for a more realistic quality assessment. We describe a concept for such a joint inversion.

[5] For this study, our motivation was to analyze global weekly GPS station coordinates and covariance matrices made available through the IGS service for the time span 26 June 1999 to 20 June 2004. One can show that estimator design and parametrization issues such as truncation degree and station distribution affect the estimation of large-scale mass redistributions like center of mass affected by loading [see *Wu et al.*, 2002] and seasonal changes of low-degree spherical harmonic coefficients from these data. Previous studies [*Blewitt et al.*, 2001; *Blewitt and Clarke*, 2003; *Wu et al.*, 2003] have used least squares estimators and impose solution constraints purely through low-degree spherical harmonic series truncation. *Wu et al.* [2003], recognizing this problem, have developed a technique where the degree of truncation in an otherwise unconstrained least squares estimator is guided by a priori statistics about GPS observation errors and aliasing errors using a load model. New in our approach is that we employ a regularized least squares estimation technique, which directly applies a physically motivated constraint only over oceanic areas, where no data are given. We can show that this technique renders the truncation problem in a less serious one. This is because one can choose a rather high degree of series expansion whereas unreasonable strong high-frequency signals are effectively damped in the inversion procedure. At the same time, unmodeled high-frequent signals are prevented from aliasing into low-degree estimates. In this case, linear combinations of spherical harmonic coefficients beyond degree 4, solved from IGS GPS data, contain significant information. Continental-scale averages at a Gaussian smoothing radius down to 2000 km exhibit visible correlations to GRACE results and those predicted from global hydrologic models. This technique might be also helpful in other inversions for spherical harmonic coefficients where discrete geophysical data are spatially restricted in coverage. On the basis of recent error assessments, we assess the contribution of adding GRACE monthly solutions in a joint inversion on the individual spherical harmonic coefficients.

2. Inverse Methodology

[6] When considering large-scale mass redistribution in the Earth system on a timescale ranging from weekly to interdecadal, it is reasonable to assume that all relevant processes occur in a thin layer at the Earth's surface. This assumption, together with a purely elastic model of the Earth's response to a unit loading mass, allows then a unique inversion of geopotential and Earth shape changes into mass redistributions. In our analysis, we assume that the gravitational and geometrical response of the Earth can be described by *Farrell*'s [1972] theory, where the load Love numbers (LLNs) only depend on the spherical harmonic degree. Whether such an approach is appropriate or not depends on the situation at hand; it might be not in a forward modeling problem when actual observations are to be corrected; but this will not be discussed in this study. Here we will consider the inverse problem where the scientific question is if a meaningful mass redistribution signal can be extracted from the data. This signal will be the sum of all atmospheric, hydrological, and oceanic loads that are not yet corrected for in the routine GRACE and GPS IGS data analysis. Whether these signals can be compared to each other or further separated depends on the quality of, e.g., atmospheric pressure models and the validity of the inverse barometric (IB) response model and is not the target of our research.

[7] Let $\Delta\sigma(\lambda, \theta)$ denote the spatially varying surface density anomaly; which has to be interpreted pointwise as a departure with respect to a multiyear mean. With the density ρ_w of seawater, assumed as 1025 kg/m^3 throughout this study, typically load thickness $T = \frac{\Delta\sigma}{\rho_w}$ is expressed as an equivalent water column. A spherical harmonic (SH) expansion for the surface density anomaly reads

$$\Delta\sigma(\lambda,\theta) = a\rho_w \sum_{l,m} \left(\Delta C^{\sigma}_{lm} \cos m\lambda + \Delta S^{\sigma}_{lm} \sin m\lambda\right) \overline{P}_{lm}(\cos\theta) \quad (1)$$

with Earth's mean radius a (6378 km), spherical harmonic degree l and order m, and SH load coefficients ΔC^{σ}_{lm} and ΔS^{σ}_{lm}. We will exclusively use fully normalized Legendre polynomials $\overline{P}_{lm}$ and spherical harmonics $\overline{Y}_{lm} = (\overline{Y}^c_{lm}, \overline{Y}^s_{lm})$, $\overline{Y}^c_{lm}(\lambda, \theta) = \overline{P}_{lm}(\cos\theta)\cos\lambda$, $\overline{Y}^s_{lm}(\lambda, \theta) = \overline{P}_{lm}(\cos\theta)\sin\lambda$ in this study, following the convention $\int_\Omega \overline{Y}_{lm}\overline{Y}_{l'm'} d\omega = 4\pi\, \delta_{ll'}\delta_{mm'}$. One relates the load SH coefficients to observable quantities, such as geoid change and crustal deformation. The choice of degree-1 LLNs implicitly defines the coordinate system to which subsequent inversions refer [*Blewitt and Clarke*, 2003]: in this study we work with $l'_1 = 0.134$, $h'_1 = -0.269$ corresponding to the center of figure (CF) frame. The CF frame, as we use it here, is conceptually defined such that the surface integral of the vector displacement field is zero, corresponding to an ideal no-net translation projected along any axis [*Blewitt*, 2003]. It will be close but not identical to realizations of the no-net translation systems where only a finite set of reference stations can be used instead of a continuous surface. On adopting the loading theory as in the work by *Farrell* [1972] and according to IERS standards, the spectral mapping for geoid, height, and lateral displacement SH coefficients is simply

$$\Delta C^{g}_{lm} = \frac{3\rho_w}{\rho_e}\frac{1}{2l+1}\left(1 + k'_l\right)\Delta C^{\sigma}_{lm} \quad (2)$$

$$\Delta C^{h}_{lm} = \frac{3\rho_w}{\rho_e}\frac{1}{2l+1}\, h'_l\, \Delta C^{\sigma}_{lm} \quad (3)$$

$$\Delta C^{\psi}_{lm} = \frac{3\rho_w}{\rho_e}\frac{1}{2l+1}\, l'_l\, \Delta C^{\sigma}_{lm} \quad (4)$$

ρ_e and ρ_w are mean density of the Earth (5517 kg/m^3) and of seawater (1025 kg/m^3), and k_l', h_l', l_l' are load Love numbers. When relating these coefficients to observations, we are now in a position to add nuisance parameters like datum offsets, rotations or a scaling. For a time-averaged geoid coefficient (like approximately over one month with GRACE), i.e.,

$$\Delta C^g_{lm} = \frac{1}{\Delta t}\int_t^{t+\Delta t} \frac{3\rho_w}{\rho_e}\frac{1}{2l+1}\left(1+k_l'\right)\Delta C^\sigma_{lm}(\tau)d\tau \quad (5)$$

or for GPS displacements in height, east, north

$$\Delta h = a\sum_{l,m}\left(\Delta C^h_{lm}\cos m\lambda + \Delta S^h_{lm}\sin m\lambda\right)\overline{P}_{lm}(\cos\theta) + \mathbf{e}_h\cdot\mathbf{\Delta x} - a\Delta s \quad (6)$$

$$\Delta e = \frac{a}{\sin\theta}\sum_{l,m} m\left(-\Delta C^\psi_{lm}\sin m\lambda + \Delta S^\psi_{lm}\cos m\lambda\right)\cdot\overline{P}_{lm}(\cos\theta) + \mathbf{e}_e\cdot\mathbf{\Delta x} + \mathbf{e}_n\cdot\boldsymbol{\epsilon} \quad (7)$$

$$\Delta n = -a\sum_{l,m}\left(\Delta C^\psi_{lm}\cos m\lambda + \Delta S^\psi_{lm}\sin m\lambda\right)\cdot\frac{\partial}{\partial\theta}\overline{P}_{lm}(\cos\theta) + \mathbf{e}_n\cdot\mathbf{\Delta x} - \mathbf{e}_e\cdot\boldsymbol{\epsilon} \quad (8)$$

Here $\mathbf{\Delta x}$, $\boldsymbol{\epsilon}$, Δs are the parameters of a residual Helmert transformation, following the IERS standard model in sign conventions, and $\mathbf{e}_h$, $\mathbf{e}_e$, $\mathbf{e}_n$ refers to the unit vectors in a local spherical frame. (Note that we understand height/east/north and vertical/horizontal generally as radial/tangential throughout this paper; that is, we work always in the spherical local frame.) Whether it is useful or harmful to estimate a residual Helmert transform, which then refers to a mean system in the considered time frame, depends on the particular context: It weakens the condition of the normal equation system somewhat, but on the other hand it gives a good indication how well pure translation and degree-1 loading can be separated for a particular station distribution and data noise realization. In general, estimated Helmert parameters are small when compared to degree-1 loading, and they do not exhibit seasonal trends as the degree-1 loading coefficients clearly do. On assuming the degree of expansion is sufficiently chosen, equations (2)–(8) constitute a Gauss-Markov model [*Koch*, 1999]

$$\mathbf{y} + \mathbf{e} = \mathbf{A}\mathbf{x} \qquad E\{\mathbf{e}\} = \mathbf{0}, \qquad E\{\mathbf{e}\mathbf{e}'\} = \mathbf{C} \quad (9)$$

where the unknown parameters ΔC^σ_{lm}, ΔS^σ_{lm} together with nuisance parameters are collected in $\mathbf{x}$. $\mathbf{A}$ refers to the design matrix, $\mathbf{y}$ holds gravity and displacement data, and $\mathbf{e}$ refers to an error vector assumed as stochastic with covariance matrix $\mathbf{C}$ ($E\{\cdot\}$ is the mathematical expectation operator). In connection with GPS data, this inverse problem has been posed originally by *Blewitt and Clarke* [2003], whereas here additionally the combination with GRACE monthly gravity fields is considered. Moreover, the estimability of parameters, the degree of truncation, and the role of other constraining operations have to be discussed in detail. In this contribution we propose a physically motivated regularization technique if GPS data only are to be inverted. With combining GRACE and GPS in the future, one would expect these problems less serious, but it might turn out that additional "empirical" parameters would have to be introduced to absorb systematic model errors. An account on the relative contribution of both data sources in a combination solution is given in section 6.

3. Estimability, Truncation, and Regularization

[8] It is obvious that one can only estimate a limited number of spherically harmonic coefficients from a limited number of observations. However, any truncation of the SH expansion leads to a potential aliasing of unmodeled higher-frequency mass redistribution signals into the solution. A method to circumvent the problem may include the choice of tailored base functions, extraction of stable linear combinations of SH coefficients (which is the essence of applying Gaussian averaging filters), and regularization. When the truncated part of the Gauss-Markov model (9) is denoted by $\tilde{\mathbf{A}}\tilde{\mathbf{x}}$, that is $\mathbf{y} + \mathbf{e} - \tilde{\mathbf{A}}\tilde{\mathbf{x}} = \mathbf{A}\mathbf{x}$, this will create a bias $\mathbf{b} = E\{\hat{\mathbf{x}} - \mathbf{x}\}$

$$\mathbf{b} = \left(\mathbf{A}'\mathbf{C}^{-1}\mathbf{A}\right)^{-1}\mathbf{A}'\mathbf{C}^{-1}\tilde{\mathbf{A}}\tilde{\mathbf{x}} \quad (10)$$

which may corrupt the least squares solution $\hat{\mathbf{x}}_{LS} = (\mathbf{A}'\mathbf{C}^{-1}\mathbf{A})^{-1}\mathbf{A}'\mathbf{C}^{-1}\mathbf{y}$. For degree-1 inversion from GPS data, *Wu et al.* [2002] have investigated this effect on the basis of different load models $\tilde{\mathbf{x}}$. One might then search for smoothed solutions of the general form

$$\hat{\mathbf{x}} = \left(\mathbf{A}'\mathbf{C}^{-1}\mathbf{A} + \alpha\Xi\right)^{-1}\mathbf{A}'\mathbf{C}^{-1}\mathbf{y} = (\mathbf{I} + \mathbf{W}_\alpha)^{-1}\hat{\mathbf{x}}_{LS} \quad (11)$$

with $\mathbf{W}_\alpha = \alpha(\mathbf{A}'\mathbf{C}^{-1}\mathbf{A})^{-1}\Xi$, with damping parameter α and regularization matrix Ξ. From the second form it becomes clear that this well-known scheme may be interpreted as a filtering operation that applies to the solved-for coefficients from a least squares solution. The estimation bias becomes

$$\mathbf{b} = \left(\mathbf{A}'\mathbf{C}^{-1}\mathbf{A} + \alpha\Xi\right)^{-1}\left(\mathbf{A}'\mathbf{C}^{-1}\tilde{\mathbf{A}}\tilde{\mathbf{x}} - \alpha\Xi\mathbf{x}\right) \quad (12)$$

for the regularized estimate. Equations (11) and (12) suggest that by choosing an appropriate regularization operator one might seek to minimize the total mean square error (propagated data error and bias) in a statistical sense, when adopting an a priori statistic about the possible load models. The mean square error [*Xu and Rummel*, 1994] will be

$$\left(\mathbf{A}'\mathbf{C}^{-1}\mathbf{A} + \alpha\Xi\right)^{-1}\mathbf{A}'\mathbf{C}^{-1}\mathbf{A}\left(\mathbf{A}'\mathbf{C}^{-1}\mathbf{A} + \alpha\Xi\right)^{-1} + \mathbf{b}\mathbf{b}' \quad (13)$$

The optimal design of regularization operators and the correct adjustment of the smoothness imposed by a priori models is, however, a challenging problem; see *Xu and Rummel* [1994] for a general discussion; a recent account in satellite gravity modeling is given by *Ditmar et al.* [2003], and for geomagnetic modeling from discrete heterogeneous data, see *Korte and Holme* [2003]. Optimization might be a topic for separate research. In section 4 we will investigate the possible aliasing error according to equation (12) simply on the basis of a simulated load model $\mathbf{x}$, $\tilde{\mathbf{x}}$, and the regularization operator chosen as described subsequently.

[9] In the present case, the land-ocean imbalance in the station distribution causes an inherent problem. Therefore we introduce an optimization principle that adds an ocean load variability constraint to the least squares objective function,

$$\mathcal{J}_\alpha = \|\mathbf{y} - \mathbf{A}\mathbf{x}\|^2_{\mathbf{C}^{-1}} + \alpha \int_{\mathcal{O}} \Delta\sigma^2 d\omega \qquad (14)$$

where $\mathcal{O}$ is the ocean area. The main purpose of our regularization operator is to allow SH representations of surface mass redistribution to follow continental signal. Oceanic mass variations are much smaller; the main signals correspond with diurnal and semidiurnal ocean tides which are corrected during the IGS GPS and GRACE data processing. A second more serious signal is that of atmospheric pressure variations. However, since we assume an inverse barometric (IB) behavior over the oceans, this is only relevant for loading over continents. Because there are very few meteorologic and GPS data over Antarctica, we extend the regularization also to this region.

[10] Numerically, our regularized inversion comes down to solving the common type of normal equation system $(\mathbf{A}'\mathbf{C}^{-1}\mathbf{A} + \alpha\Xi_{\mathcal{O}})\hat{\mathbf{x}} = \mathbf{A}'\mathbf{C}^{-1}\mathbf{y}$. The particular regularization matrix $\Xi_{\mathcal{O}}$ associated with (14) equals the Gram matrix that appears in the base function orthonormalization method and the product-sum formulation of spherical harmonics. Computing its entries requires in principle either a spherical harmonic analysis of the harmonics $\overline{Y}_{lm}$ masked with the ocean function $\mathcal{O}$ (1 over ocean and 0 over land),

$$\begin{aligned}\Xi_{\mathcal{O};lm,l'm'} &= \int_\omega O\,\overline{Y}_{lm}\,\overline{Y}_{l'm'}\,d\omega \\ &= \frac{1}{4\pi}\sum_{l'',m''}\overline{O}_{l''m''}\int_\Omega \overline{Y}_{lm}\overline{Y}_{l'm'}\overline{Y}_{l''m''}d\omega \end{aligned} \qquad (15)$$

or the evaluation of recursive algorithms involving Clebsch-Gordon coefficients. For such recursions, see *Hwang* [1995], *Pail et al.* [2001], and *Blewitt and Clarke* [2003, and references cited therein]. We chose to implement the spherical harmonic analysis method, requiring only standard algorithms after a suitable discretization on regular grids. The parameter α controlling the weight of the constraint against the data fit is sometimes determined from trade-off investigations, but we propose to apply a discrepancy principle here: by adjusting α we force the total spatial variability of the inversion result, on average with respect to time, to an average value obtained from a geophysical model time series (see section 5). The matrix $\Xi_{\mathcal{O}}$, on the other hand, is determined by the constraining norm in equation (14). Other reasonable principles, which all share the property that they force smoothness of the inversion outcome over oceanic regions, include constraining the surface gradients $(\nabla^*\Delta\sigma)^2$ and the surface Laplacian $(\Delta^*\Delta\sigma)^2$ of the mass redistribution instead of the total variability $\Delta\sigma^2$. It is not difficult to derive the corresponding regularization matrices for these cases, which contain additional degree-dependent factors in (15).

[11] Our regularized inversion operator differs thus significantly from the constrained inversion scheme proposed by *Blewitt and Clarke* [2003]. In their methodology, an unconstrained low-degree least squares inversion $(\mathbf{A}'\mathbf{C}^{-1}\mathbf{A})\hat{\mathbf{x}}_{LS} = \mathbf{A}'\mathbf{C}^{-1}\mathbf{y}$ initially provides the SH coefficients of the total mass redistribution. Then, postulating that the marine geoid and sea bottom deformation changes associated with the mass redistribution must correspond point-wise to relative sea level changes (assuming thus that the ocean is in hydrostatic equilibrium, responding to a forcing by continental loads), sea level SH coefficients are split off the estimated mass redistribution SH coefficients using the product-to-sum transformation of spherical harmonics. The remaining part is ascribed to the land part of the mass redistribution SH coefficients in their analysis. Oceanic and continental loads are computed spatially using "quasi-spectral" SH coefficients, which are obtained from SH coefficients through projection by $\Xi_{\mathcal{O}}$. Numerical results were provided for truncation degrees 1. Conversely, in our methodology a physically motivated constraint about possible oceanic loads is already incorporated in the estimation scheme; whereas hydrostatic equilibrium is not postulated explicitly.

4. Simulation Analysis of the Spatial Aliasing Bias

[12] In order to investigate the possible spatial aliasing bias according to equation (12), we have conducted a simple simulation. Our load model consists of a spherical harmonic expansion complete to degree 90, derived from converting the August 2003 GRACE atmosphere-ocean de-aliasing (AOD) model from the GRACE project into a load expansion and adding the corresponding CPC land hydrology anomaly model [*Fan and van den Dool*, 2004]. Thus, for August 2003, it represents the combination of atmospheric pressure, the response of a barotropic ocean model, and the hydrologic variation with respect to a multiyear mean. However, the details of its creation are in fact less important, as long as the model provides a realistic load distribution, because the purpose of this model is to serve as the truth model within the simulation. The latitude-weighted global RMS of the load distribution is 4.6 cm, with peak values of about 35 cm. We apply this model to generate horizontal and vertical deformation data, by means of equations (6)–(8), for the same 142 IGS station positions that we extract in the analysis of real data from the IGS combination SINEX file for week 1230 (August 2003), as described in section 5. RMS of the simulated deformation vector components are 2.8/0.3/0.4 mm in height/east/north direction from the full degree-90 expansion; the aliasing signal part above degree 7 (the maximum degree that we solve for in the inversion) contributes to 1.2/0.2/0.2 mm RMS. No stochastic errors are introduced. In the light of equation (12), the truth model consists of two parts: $\mathbf{x}$ holds those coefficients complete to degree 7 that we estimate with a possible regularization bias from the simulated data, in $\tilde{\mathbf{x}}$ are those above the truncation degree in the analysis causing a spatial aliasing bias.

[13] For the first simulation experiment, the data have been taken from the degree-7 truth expansion $\mathbf{x}$, with all deformation component data weighted equally. The simulated problem is consistent in algebraic sense, i.e., the error

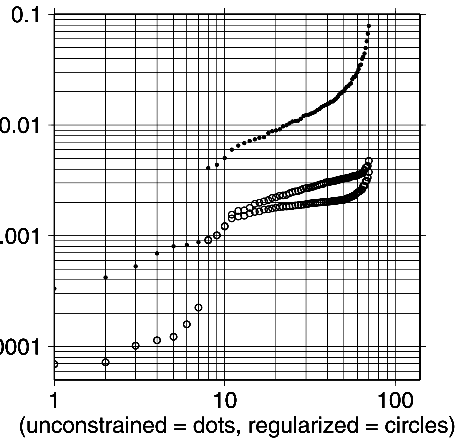

Figure 1. Square root of eigenvalues of the inverse normal matrix, unconstrained (dots) and regularized (circles, for the two damping parameter used in the real-data analysis) inversion, in m. Inversion for degree-7 expansion and Helmert parameters.

vector **e** in equation (9) vanishes. The unconstrained solution, with an

$$\mathrm{RMS} = a\sqrt{\frac{1}{\#\mathrm{coeff}}\sum_{l,m}\left(\Delta C^{\sigma}_{lm} - \widehat{\Delta C}^{\sigma}_{lm}\right)^2 + \left(\Delta S^{\sigma}_{lm} - \widehat{\Delta S}^{\sigma}_{lm}\right)^2}$$

of spherical harmonic coefficient errors of less than 0.7 mm, appears indeed close to the truth model; which is an expected result because the station distribution oversamples the spherical harmonic expansion. Care has to be exercised when interpreting relative errors: even in this aliasing-free case they may easily reach 200% due to the smallness of some coefficients. The fact that there are errors at all in the unconstrained inversion from error-free data can be attributed to the fast decay rate of the Love numbers and the inhomogeneous station distribution, which in combination cause the normal matrix to become ill conditioned. The errors in the constrained solution (RMS spherical harmonic coefficient error of less than 1.0 mm) equal to the bias **b** in equation (12) in the case $\tilde{\mathbf{x}} = \mathbf{0}$. This solutions should be seen as a reference solution with respect to the aliasing problem, which we consider subsequently.

[14] For the second experiment, the data have been taken from the degree-90 truth expansion, with the inversion complete up to degree 7. An aliasing term $\tilde{\mathbf{x}}$ of realistic magnitude is thus present in this simulation. Equally weighting all data is, however, not realistic, and it is not what happens in the real-data inversion. We have therefore applied a real, dense GPS variance covariance matrix **C** from the SINEX file of GPS week 1230 for decorrelating the data. In Figure 1 we draw in log-log scaling the square root of the inverse normal matrix eigenvalues corresponding to the least squares solution and to two regularized solutions. Because all estimated parameters are scaled to metric quantities (in [m]), these can be directly compared in their contribution to the overall error covariance. Helmert and degree-1 parameters are estimated unconstrained in our method, corresponding to the first ten eigenvalues in Figure 1, and we can see how SH coefficient contributions of higher degree are progressively damped. The two regularization parameter $\alpha' = 0.3 \times 10^5$ and $\alpha'' = 0.9 \times 10^5$ used in this simulation are the same that we applied in the real-data analysis; see section 5 for their derivation using different external geophysical models. We find the RMS of SH coefficient errors to about 2.5 mm for the unconstrained inversion, about 1.8 mm for the regularized inversion with α', and about 2.1 mm for the regularized inversion with α''. The least squares solution exhibits significant oscillations, even in regions sufficiently populated with data, which we explain by the fact that aliasing errors get amplified in the inversion procedure. Regularization smoothes these oscillations efficiently. However, most of the larger features of the truth signal are still preserved. Like in all inversions from the degree-90 data, there appears a problem with North America (large high-frequency signal and many stations at west coast United States/Canada). This is particularly interesting because a similar pattern can be observed in the comparisons of real-data inversion and the land hydrology model (section 5). The maximum error in degree-1 coefficients here is 5.8 mm (c_{10}), corresponding to an error of $\sqrt{3}(\rho_w/\rho_e)$ = 1.9 mm in north-south (interhemisphere) geocenter motion. Finally, for comparison, we have run two simulations where the constraints are applied purely through truncating the series expansion. The same data as in the previous experiment have been used, but the inversion is solved for either up to degree 2 or up to degree 4. In the first case the RMS of SH coefficient errors for degrees 1 and 2 was 1.6 mm, whereas we found 1.0 mm (α') and 1.2 mm (α'') from the regularized degree-7 inversions. In the second case the RMS including degrees up to 4 was 1.4 mm, with 1.2 mm (α') and 1.4 mm (α'') from the regularized degree-7 inversions. This shows clearly that degree-2 inversions may suffer considerably from aliasing, and that constrained degree-7 solutions may perform better for degrees $\leq$4 than the unconstrained degree-4 solution.

5. Analysis of IGS GPS Coordinates

[15] We have applied our analysis to weekly IGS GPS combination coordinate sets spanning 1999.5–2004.5 (26 June 1999 to 20 June 2004), obtained from the IGS ftp site as SINEX files (igsyyPwwww.snx) and equipped with full variance-covariance matrices. In total 158 sites which contribute for more than 2 years in the mentioned time span and for whose time series visible inspection did not reveal steps were selected. Linear station movements have been removed, and all time series are centered about the mean. Note further that since the summer of 2001 there is a significant increase in the number of sites.

[16] Within the inversion, we solved for a maximum resolution of l = 7 in the spherical harmonic expansion for each week. Regularization with the ocean damping matrix $\Xi_{\mathcal{O}}$, and using two different values for the damping parameter was applied: either $\alpha'' = 0.9 \times 10^5$ corresponding on average with respect to time to an a posteriori total spatial variability of $\int_{\mathcal{O}} \widehat{\Delta\sigma}^2 d\omega = \hat{\mathbf{x}}'\Xi_{\mathcal{O}}\hat{\mathbf{x}}$ of $(0.014\ \mathrm{m})^2$ (an average value taken from an ECCO ocean bottom pressure model [*Stammer et al.*, 1999]); or $\alpha' = 0.3 \times 10^5$ corresponding on average to $\int_{\mathcal{O}} \widehat{\Delta\sigma}^2 d\omega = \hat{\mathbf{x}}'\Xi_{\mathcal{O}}\hat{\mathbf{x}}$ of about

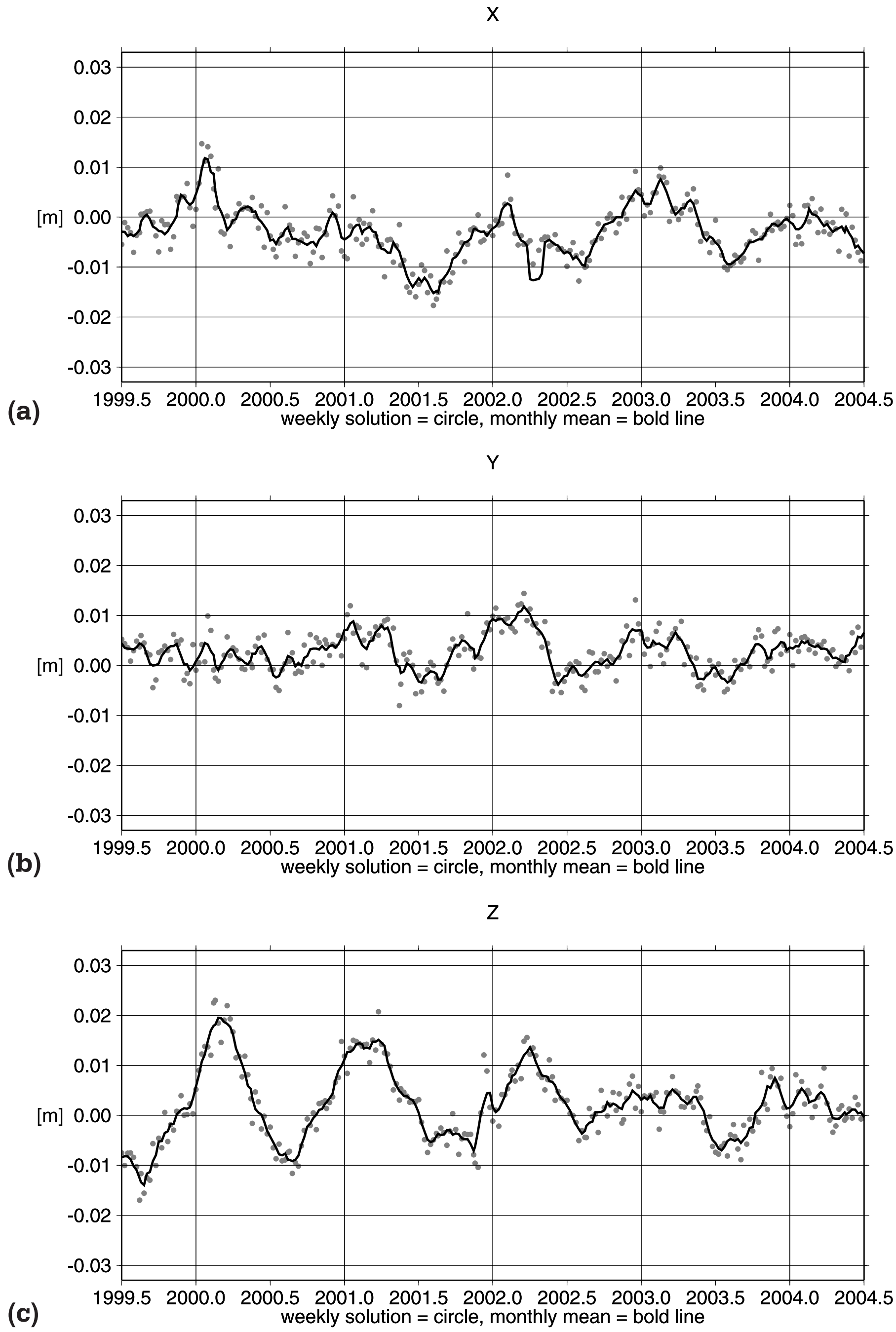

Figure 2. Load moment expressed as CF frame variation [m] with respect to CM from GPS inversion, in X, Y, Z direction (CF center of figure system, CM joint center of mass of Earth and load). Weekly estimates (dots), and running 30 day mean (line).

$(0.032\ \mathrm{m})^2$ (the value following from an analysis of the 18 published GRACE gravity field models from University of Texas Center of Space Research, projected to mass variability by inverting SH coefficients through equation (2)). These "calibration" values from the geophysical models follow from spherical harmonic expansion and expressing the total spatial variability in the same spectral band where the inversion is to be constrained. Loosely speaking, we can choose between constraining our inversion model to an oceanic spatial variability derived from an ocean model or from the satellite gravity estimates. As with the simulation, we exclude degree-1 deformation from the regularization. Furthermore, we rejected some 1% of observations where either height, east or north displacements did not pass a statistical test in the unconstrained analysis; with the test criterium chosen to meet no more than 5% probability of failing to reject a true outlier. Figure 2 shows the estimated load moment **m** evolution, expressed as a variation of the CF frame with respect to the center of mass of Earth plus load (CM) system. The

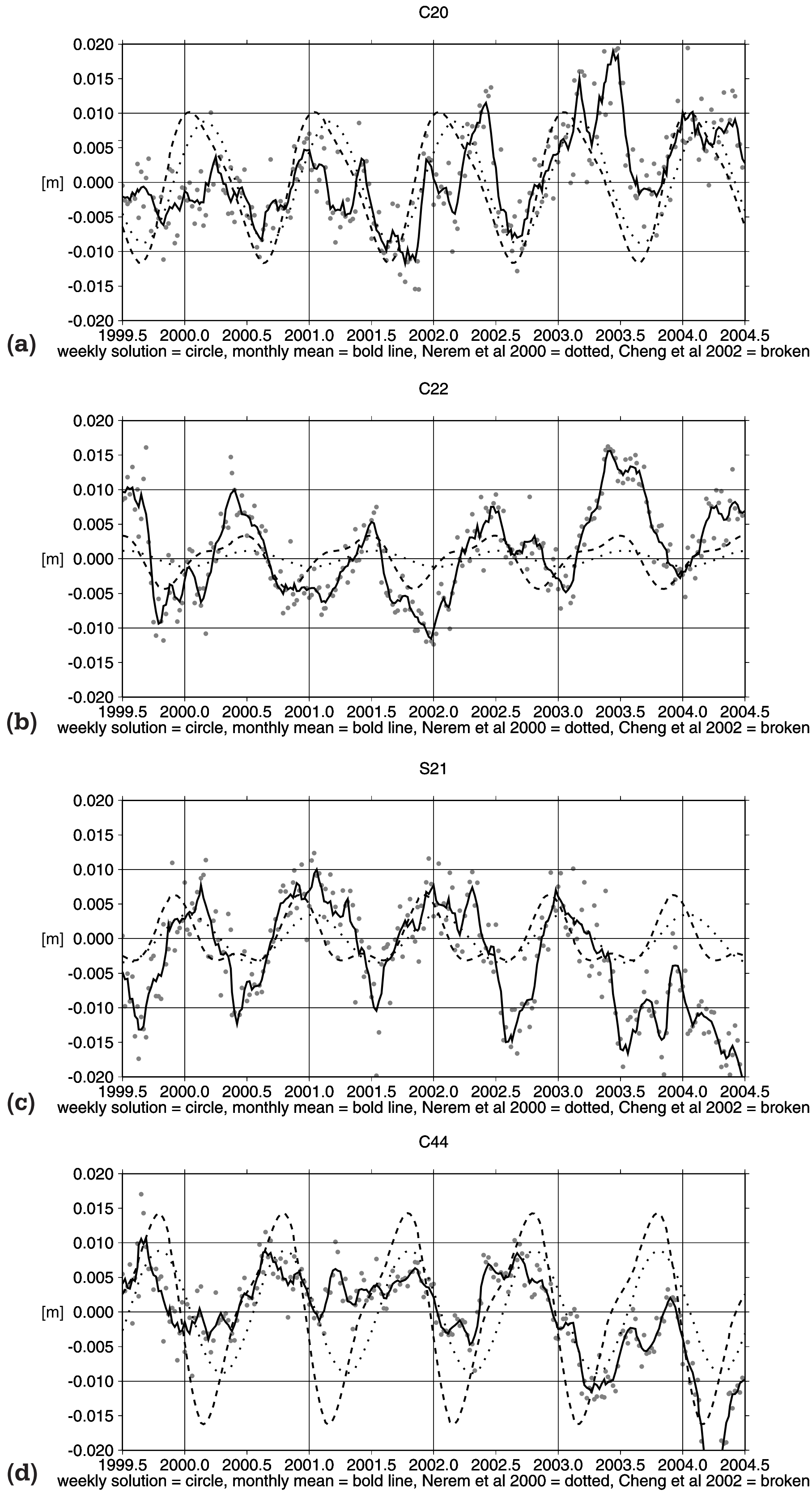

Figure 3. Low-degree load harmonic coefficients [m] from GPS inversion (α' derived from GRACE time-variable gravity models). Weekly estimates (dots), running 30 day mean (line), and two models from SLR analyses.

Table 1. Annual Amplitude/Phase for Low-Degree Load Harmonic Coefficients[a]

	Unconstrained	α'	α''	*Nerem et al.* [2000]	M. K. Cheng et al. (unpublished manuscript, 2002)
ΔC_{20}^{σ}	6.2/40	4.6/89	3.4/90	8.8/56	10.3/31
ΔC_{22}^{σ}	9.7/142	6.5/170	4.7/172	1.2/187	3.2/134
ΔS_{21}^{σ}	14.1/359	6.3/384	4.5/20	3.5/8	4.2/332
ΔC_{44}^{σ}	16.2/284	5.6/269	3.4/266	8.9/287	13.4/254

[a]Annual amplitude is in mm and phase is counted in days from 1 January from GPS inversion (unconstrained, and with $\alpha' = 0.3 \times 10^5$ derived from GRACE and $\alpha'' = 0.9 \times 10^5$ derived from ocean bottom pressure model) and after *Nerem et al.* [2000] and M. K. Cheng et al. (unpublished manuscript, 2002).

load moment vector is defined as by *Blewitt* [2003] (equation (9)). This means, the

$$
\begin{aligned}
X &= \frac{1}{M}\mathbf{m}_x = \frac{1}{M}\frac{4\pi a^4 \rho_w}{3}\Delta C_{11}^{\sigma} \\
Y &= \frac{1}{M}\mathbf{m}_y = \frac{1}{M}\frac{4\pi a^4 \rho_w}{3}\Delta S_{11}^{\sigma} \\
Z &= \frac{1}{M}\mathbf{m}_z = \frac{1}{M}\frac{4\pi a^4 \rho_w}{3}\Delta C_{10}^{\sigma}
\end{aligned}
\tag{16}
$$

are displayed. 1-sigma standard deviations for the individual weekly estimates are about 4–5 mm. The period 1999.5–2001.0, after scaling displacements by Earth's mass M = 6.0×10^{24} km, fits very close to Figure 1 from *Blewitt et al.* [2001], who solved for degree-1 only. In comparison with the results of *Wu et al.* [2003] for 1999.5–2002.0, we find similarities notably in Z, but our amplitudes are significantly larger within this period although they decrease for more recent years. We find a yearly amplitude (in mm) and phase (day of maximum amplitude, counted from 1 January) of 3.9/23 in X, 2.7/26 in Y, 7.6/58 in Z direction. Dropping the residual Helmert parameters (whose values are generally estimated to be below the 1 mm level) from the estimation alters these values to 5.4/25 in X, 1.1/323 in Y, 5.9/52 in Z. Estimated statistical correlations vary between −0.1 and −0.6 in our regularized inversion, depending on site distribution and coordinate axis. One should add that these degree-1 results appear as almost insensitive with respect to the specifically chosen constraint, the chosen station subset (we used more than twice the number of stations that *Blewitt et al.* [2001] used), or the degree of series truncation, as long as one applies a reasonable constraint at all when extending the truncation degree. They are, on the other hand, sensible toward the chosen degree-1 LLNs and the underlying reference frame concept.

[17] In Figure 3 we show some estimated low-degree spherical harmonic coefficients for the regularization parameter derived using time-variable satellite gravity models. For comparison, two spherical harmonic models for annual and semiannual gravity changes from SLR analysis [*Nerem et al.*, 2000; *Cheng et al.*, 2002] have been projected to loading mass variations and included in Figure 3. Table 1 summarizes annual amplitude and phase for these low-degree coefficients, where we included results obtained using both constraints α' and α'' as well as from the unconstrained inversion for completeness. Obviously, the amplitudes are indeed somewhat sensitive to the particular choice of the constraint, whereas the annual phase in our estimates agrees generally quite well with the SLR results. Differences between the second and third column indicate to which extent our analysis results depend on external information introduced through the damping. For higher degrees ($l > 2$) there is typically less power in our regularized estimates than in those obtained from SLR analyses, as shown here for $l = m = 4$. Moreover, our results suggest that energy is transferred from the north-south (Z) annual oscillation to C_{20}. This pattern reappears when we repeat our computation with different station subsets, so it is probably not related to the increasing number of IGS stations. However, care has to be exercised when judging individual spherical harmonic coefficients, as the simulations in section 4 have shown.

[18] The weekly SH coefficients are corrected for known oceanic and atmospheric mass variations. We assumed an inverted barometer response over the oceans and continental air pressure loading using the National Center for Earthquake Prediction (NCEP) reanalysis air pressure data. Several versions have been implemented and our current results are based upon a gravitational consistent theory as described by *Wahr* [1982]. We did not obtain significant differences when applying the standard local IB correction whereby a constant reference pressure is assumed, the modified dynamical IB correction that allows variations in this reference pressure so that there are no net mass changes over the oceans (recommended as an option by TOPEX/Poseidon and JASON science working team), or when applying the theory of *Wahr* [1982] that combines air pressure loading on land and sea level variations in a gravitational consistent manner. The corrected GPS inversions should then basically be comparable to what GRACE delivers at the large spatial scales. Then, we derived the annual cosine and sine modes from the last two years of our analysis (for better comparison with the GRACE solutions). We represent annually varying spatial mass distribution in Figure 4a graphically at resolution of $l = 3\ldots 6$, derived from GPS (using the damping α' from adjusting the oceanic spatial variability to GRACE). For comparison and validation, Figure 4b gives the corresponding annual surface mass change ($l = 3\ldots 6$), as computed from the CPC land hydrology model, and Figure 4c shows these changes as derived from the CSR GRACE level 2 product (when referred to a mean GRACE solution). Note that no spectral filtering has been applied to the GRACE fields. Annual mass changes from GPS inversion appear generally less pronounced than the GRACE results, and the separation between strong sine and weak cosine mode is less clear. However, the visual correspondence between our inversion, the hydrology model, and the GRACE-derived solutions is still striking, given the relatively sparse data distribution. We do not attempt any geophysical interpretation of the misfits.

[19] Finally, we have computed time series of large-scale spatial averages of mass distribution for the individual continental surface of Europe/Asia, Africa, Australia, North America and South America (see Figure 5) from our inversion. Also for these graphs the atmospheric pressure contribution has been removed from the GPS inversion results in a postanalysis step. Corresponding time series

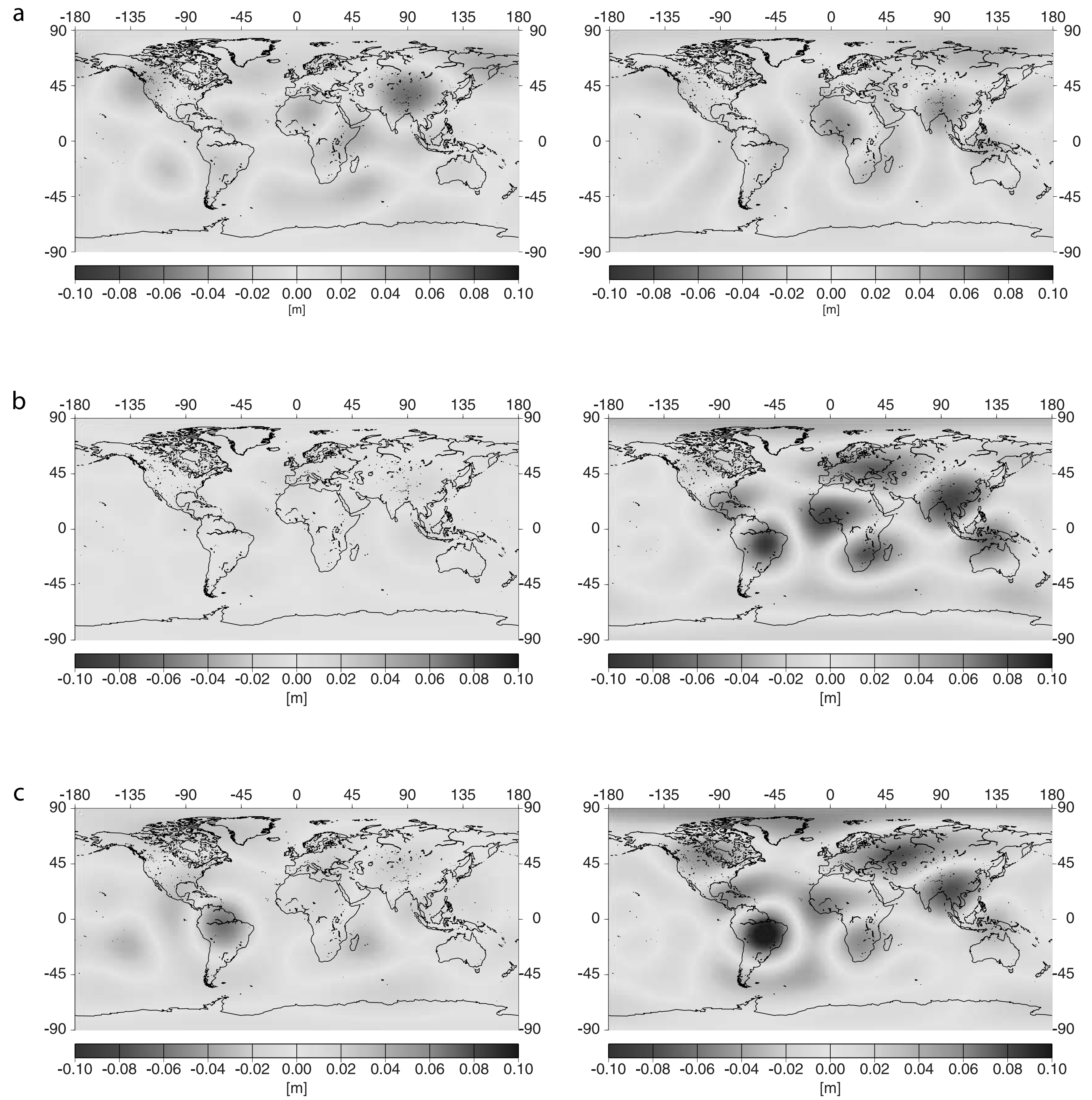

Figure 4. Annual surface density variation in equivalent water height [m], (a) from GPS inversion, $l = 3\ldots6$ (atmospheric effect removed (from NCEP)), (b) from CPC land hydrology model, $l = 3\ldots6$, and (c) from CSR GRACE models, $l = 3\ldots6$. (left) Cosine mode, (right) sine mode. See color version of this figure at back of this issue.

from the CPC models [*Fan and van den Dool*, 2004] and monthly results from the GRACE project (CSR fields) are included for comparison. Here, all spatial averages are obtained through applying an identical Gaussian filter procedure with averaging radius of 2000 km to spherical harmonic expansions truncated at degree $l = 7$ (the maximum resolution within the GPS inversion), in order to avoid Gibbs effects and to reduce the noise. These filter coefficients suppress more than 92% of the unmodeled signal at degrees >7. The GPS and GRACE curves for Europe and Asia fit quite well in amplitude and phase, an offset may be identified for Africa (still remarkable correspondence seen the few contributing GPS station), but no similarity appears between GPS inversion and GRACE-derived results for North America. For South America with its large hydrologic basins exposing a pronounced signal which is clearly identifiable in GRACE solutions [*Tapley et al.*, 2004], GPS inversions appear phase-lagged and of smaller amplitude. Adding these results up, including degree-1 harmonics and scaling appropriately by the total continental surface area times seawater density, represents the exchange of water mass between these five continents and all those

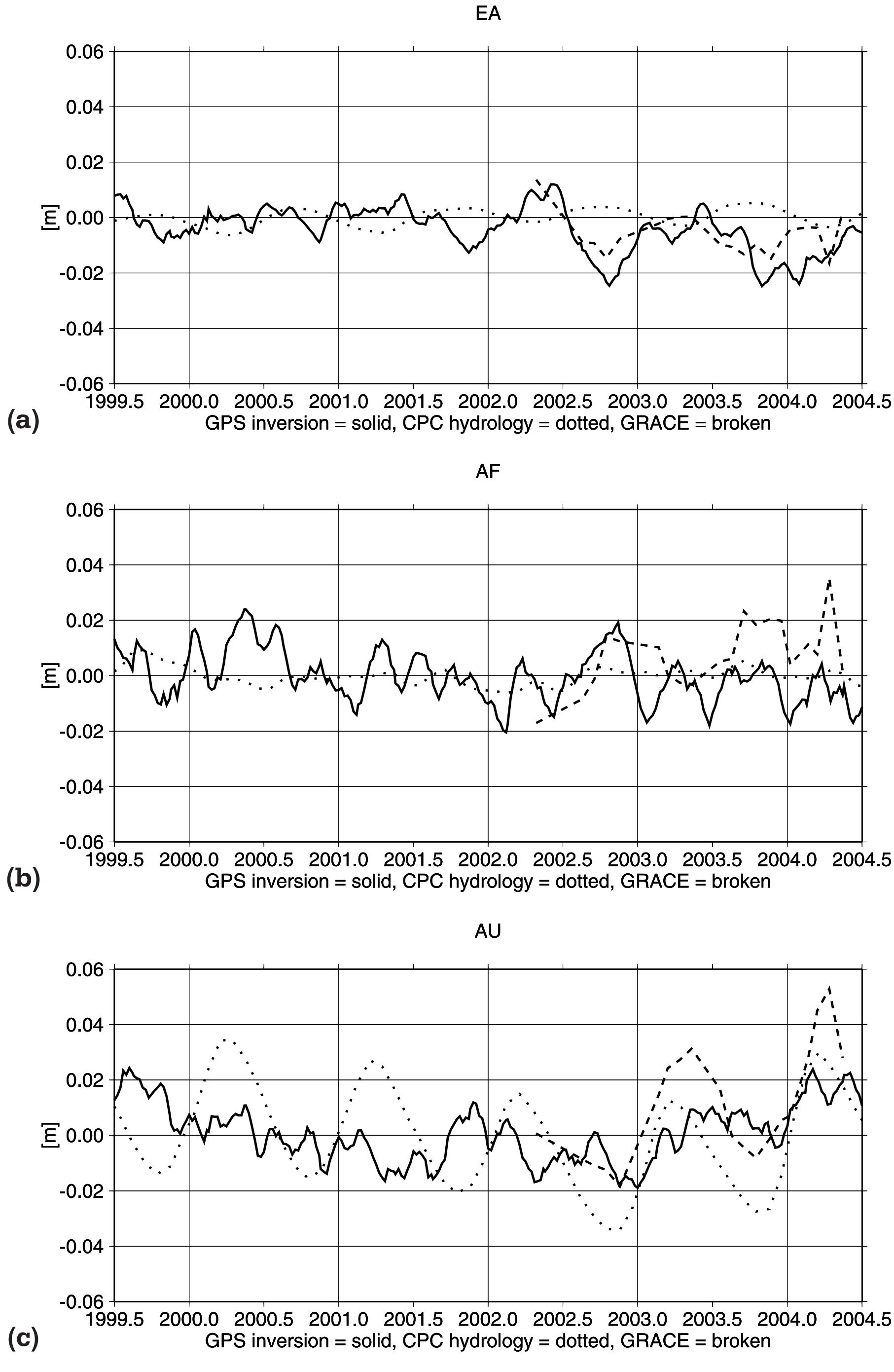

Figure 5. Monthly surface density variation in equivalent water height [m] averaged over continental regions (EA, Europe plus Asia; AF, Africa; AU, Australia; NA, North America; SA, South America). GPS inversion (running 30 day mean, solid line), CPC hydrology model (dotted line), and GRACE (dashed line). Gaussian smoothing with 2000 km averaging radius applied. Degrees 2. . .7 used exclusively. Atmospheric effect removed (from NCEP).

water storage systems which do not load the continental surface. When we assume that the atmosphere plays a minor role in the water exchange, this would be the ocean (including the arctic region) and Antarctica. We derive an annual amplitude of 2.1×10^{15} kg with a minimum in early September for mass exchange, noting that the degree-1 terms (something which is not provided with GRACE solutions) dominate this result. However, a clear decrease in amplitude can be observed, so that this value can only represent a mean in the time frame 1999.5–2004.5. *Blewitt and Clarke* [2003] found an annual amplitude of 2.9×10^{15} kg with a minimum in late August from analysis of data spanning the period 1996.0–2001.0; however, their methodology differs significantly from the one presented here. We conclude that there appear differences in amplitude and phase between GRACE results and GPS inversions, which are probably too large to be considered as purely stochastic. It is tempting to apply a rigorous joint inversion of the

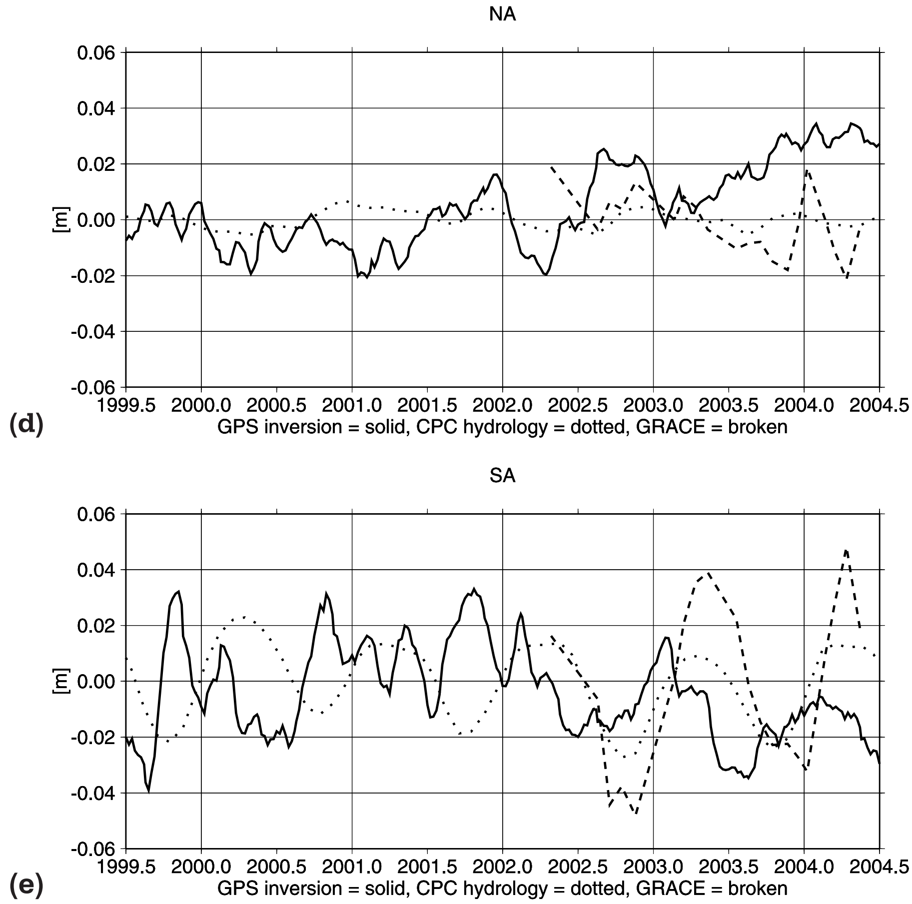

Figure 5. (continued)

two data sources, combining equations (5)–(8), but such systematic differences should be investigated first before being masked by an adjustment procedure. However, in section 6 we will investigate which spherical harmonic coefficients would gain in such a joint inversion based on an error assessment.

6. Simulation of GRACE Full Covariance and Relative Contribution

[20] What would be the contribution of GPS in a joint monthly inversion, that is, when one combines monthly GRACE gravity coefficients (5) and GPS station displacements (6), (7), and (8) from four consecutive weeks? Note that the GRACE accuracy for 2003 is ranked significantly better than that for 2002. In order to assess this question, we have therefore used the GPS variance-covariance matrices $\mathbf{C}^{h,\psi}$ that we extracted from the GPS week 1180 (August 2002) and 1230 (August 2003) SINEX files for the computation in section 5 together with the calibrated 1-sigma information of the corresponding monthly CSR GRACE solutions [*Tapley et al.*, 2004]. However, because the GRACE files are not given with a full covariance matrix (there is no correlation information), we have built up such matrices $\mathbf{C}^g$ from simulation with the energy balance approach for gravity field recovery [*Jekeli*, 1999] and 30 days of simulated orbits [*Ilk et al.*, 2003] and scaled subsequently coefficient-wise to match the actual CSR calibrated coefficient standard deviations. The contribution of GRACE can then be judged by evaluating the partial redundancy for a particular gravity coefficient ΔC^g_{lm} [*Koch*, 1999], and the contribution of the GPS site distribution to ΔC^σ_{lm} is $1 - q_{lm}$,

$$q_{lm} = \mathbf{a}^{g\prime}_{lm} \left(\mathbf{A}^{g\prime} \mathbf{C}^{g-1} \mathbf{A}^g + \mathbf{A}^{h,\psi\prime} \mathbf{C}^{h,\psi-1} \mathbf{A}^{h,\psi} \right)^{-1} \mathbf{A}^{g\prime} \mathbf{C}^{g-1} \mathbf{e}_{lm} \quad (17)$$

where $\mathbf{a}^g_{lm}$ is the corresponding column of the design matrix, and $\mathbf{e}_{lm}$ a vector with 1 in the position corresponding to l, m and 0 elsewhere.

[21] The projections (Figure 6) show clearly that the gain through adding GPS lies in the very low degrees and to some extent in sectorial and near-sectorial harmonics. There is a 60% contribution up to degree 4, and about 30% contribution up to higher degrees in sectorial and near-sectorial coefficients. Of course, our methodology here assumes that the data errors are perfectly modeled through the covariance matrices $\mathbf{C}^g$ and $\mathbf{C}^{h,\psi}$ and that no model errors exist, which is probably not the case in reality. Also, with increasing GPS site density and increasing GRACE accuracy such projection will have to be reconsidered.

7. Conclusions

[22] We have analyzed publicly available weekly IGS GPS time series from the years 1999.5–2004.5 for mass

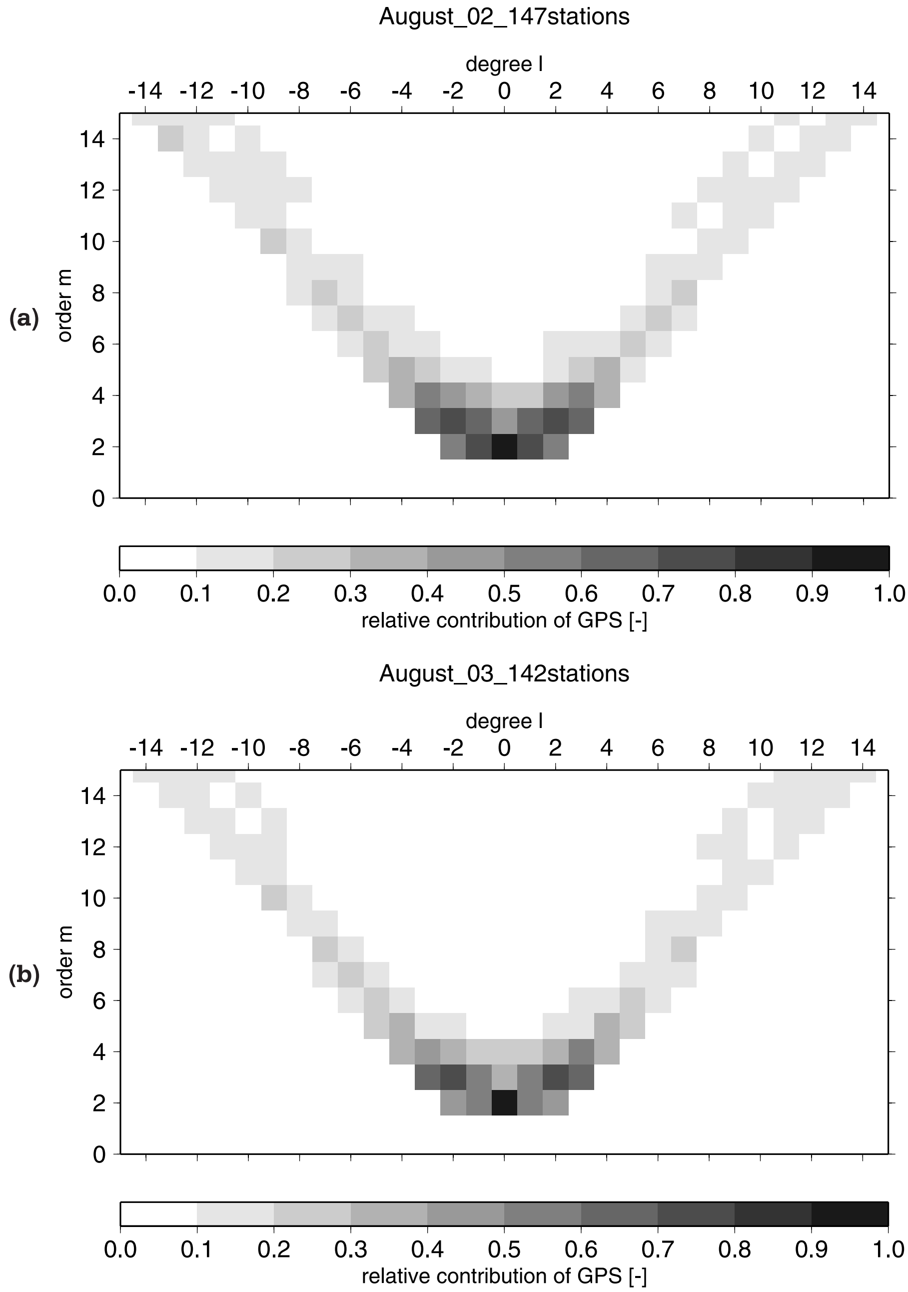

Figure 6. Projection of the relative contribution of GPS (a) August 2002 and (b) August 2003 in a joint 4-week GRACE-GPS inversion; 1, coefficient completely determined from GPS; 0, from GRACE.

redistribution through loading inversion. Truncation and regularization issues affect the estimation of low-degree mass changes; due to nonhomogeneous site distribution and the amplification of errors. Our results show that a regularized inversion technique, which takes only the physically motivated constraint of limited oceanic variability via the IB assumption into account, renders this parametrization problem into a less significant one. Spherical harmonic coefficients well beyond degree 4 appear to contain significant information. We can show that after removing the contribution ascribed to atmospheric pressure loading following a gravitationally consistent IB theory, estimated annual variations of continental-scale mass distributions exhibit pattern similar to those observed with GRACE and predicted by a global hydrology model, although systematic differences appear to be present. Further research should concentrate on identifying these systematics. For instance, in the present analysis we do not take possible systematic or seasonal error sources in the GPS system into account. On the other hand, it is difficult to quantify the reliability of global hydrologic models and even the "calibrated" error estimates from the GRACE project are hard to validate. Improvements with GRACE modeling and data processing methodology will probably change this picture, but dependent on the quality of future reprocessed monthly solutions, there might be still a potential for combination with GPS. Moreover, reliable GPS time series date much longer back in the past than GRACE is in existence.

[23] One might argue that in our method the physical constraint provides a rather coarse description of the ocean dynamic behavior, and that one could go one step further and penalize the deviations from a seasonal mean sea level model instead of the absolute oceanic mass variability. Ocean dynamics can in fact be introduced into the inversion scheme on various levels of information content: with no constraint at all on one end of the scale and a weighted least squares inversion combining an ocean model with GPS and/or GRACE on the other end. Naturally, with increasing the importance of prior information the dependence on the prior model of ocean dynamics will increase. For the moment we have chosen a rather conservative approach, but more elaborated constraining mechanisms are under investigation. Also the question, whether to include frame-dependent degree-1 load coefficients into the constraint would improve the solutions, is being investigated. An argument for the current approach is that we can derive the weight of the constraint alternatively from GRACE.

[24] Finally, the method as outlined in this article may be extended to applying additional constrains over land areas, for example to deal with areas of sparse GPS coverage or with GRACE errors which increase strongly at higher degrees of truncation. In fact, applying Gaussian-type averages as is common in the interpretation of GRACE gravity fields is just another way of filtering the unconstrained inversion outcome (equation (11)).

[25] **Acknowledgments.** We acknowledge the use of IGS GPS station coordinate SINEX files made publicly available through ftp. Thanks go also to the GRACE project for using their level 2 products. Finally, we thank Xiaoping Wu and an anonymous referee for providing very constructive reviews.

References

Blewitt, G. (2003), Self-consistency in reference frames, geocenter definition, and surface loading of the solid Earth, *J. Geophys. Res.*, *108*(B2), 2103, doi:10.1029/2002JB002082.

Blewitt, G., and P. Clarke (2003), Inversion of Earth's changing shape to weigh sea level in static equilibrium with surface mass redistribution, *J. Geophys. Res.*, *108*(B6), 2311, doi:10.1029/2002JB002290.

Blewitt, G., D. Lavallee, P. Clarke, and K. Nurutdinov (2001), A new global mode of Earth deformation: Seasonal cycle detected, *Science*, *294*, 2342–2345.

Chao, B. (2005), On inversion for mass distribution from global (time-variable) gravity field, *J. Geodyn.*, *39*, 223–230, doi:10.1016/j.jog.2004.11.001.

Cheng, M. K., B. Gunter, J. C. Ries, D. P. Chambers, and B. D. Tapley (2002), Temporal variations in the Rarth's gravity field from SLR and CHAMP GPS data, in *Gravity and Geoid 2002, 3rd Meeting of the International Gravity and Geoid Commission*, edited by I. N. Tziavos, pp. 326–331, Ziti, Thessaloniki, Greece.

Ditmar, P., J. Kusche, and R. Klees (2003), Computation of spherical harmonic coefficients from gravity gradiometry data to be acquired by the GOCE satellite: Regularization issues, *J. Geod.*, *77*(7–8), 465–477.

Fan, Y., and H. van den Dool (2004), Climate Prediction Center global monthly soil moisture data set at 0.5° resolution for 1948 to present, *J. Geophys. Res.*, *109*, D10102, doi:10.1029/2003JD004345.

Farrell, W. E. (1972), Deformation of the Earth by surface loads, *Rev. Geophys.*, *10*(3), 761–797.

Hwang, C. (1995), A method for computing the coefficients in the product–sum formula of associated Legendre functions, *J. Geod.*, *70*, 110–116.

Ilk, K. H., P. Visser, and J. Kusche (2003), Satellite gravity field missions, Final Report Special Commission 7, General and technical reports 1999–2003, Sapporo, *Trav. IAG 32*, Int. Assoc. of Geod., Paris.

Jekeli, C. (1999), The determination of gravitational potential differences from satellite-to-satellite tracking, *Celestial Mech. Dyn. Astron.*, *75*, 85–100.

Koch, K.-R. (1999), *Parameter Estimation and Hypothesis Testing in Linear Models*, Springer, New York.

Korte, M., and R. Holme (2003), Regularization of spherical cap harmonics, *Geophys. J. Int.*, *153*, 253–262.

Nerem, R. S., R. J. Eanes, P. F. Thompson, and J. L. Chen (2000), Observations of annual variations of the Earth's gravitational field using satellite laser ranging and geophysical models, *Geophys. Res. Lett.*, *27*(12), 1783–1786.

Pail, R., G. Plank, and W.-D. Schuh (2001), Spatially restricted data distributions on the sphere: The method of orthonormalized functions and applications, *J. Geod.*, *75*, 44–56.

Stammer, D., et al. (1999), The consortium for estimating the circulation and climate of the ocean (ECCO)—Science goals and task plan, *ECCO Rep. 1*, ECCO Consort., Scripps Inst. of Oceanogr., La Jolla, Calif. (Available at http://www.ecco-group.org)

Swenson, S., and J. Wahr (2002), Methods for inferring regional surface-mass anomalies from Gravity Recovery and Climate Experiment (GRACE) measurements of time-variable gravity, *J. Geophys. Res.*, *107*(B9), 2193, doi:10.1029/2001JB000576.

Tapley, B. D., S. Bettadpur, J. C. Ries, P. F. Thompson, and M. M. Watkin (2004), GRACE measurements of mass variability in the Earth system, *Science*, *305*, 503–505.

Wahr, J. (1982), The effects of the atmosphere and oceans on the Earth's wobble—1. Theory, *J. R. Astron. Soc.*, *70*, 349–372.

Wu, X., D. F. Argus, M. B. Heflin, E. R. Ivins, and F. H. Webb (2002), Site distribution and aliasing effects in the inversion for load coefficients and geocenter motion from GPS data, *Geophys. Res. Lett.*, *29*(24), 2210, doi:10.1029/2002GL016324.

Wu, X., M. B. Heflin, E. R. Ivins, D. F. Argus, and F. H. Webb (2003), Large-scale global surface mass variations inferred from GPS measurements of load-induced deformation, *Geophys. Res. Lett.*, *30*(14), 1742, doi:10.1029/2003GL017546.

Xu, P., and R. Rummel (1994), Generalized ridge regression with applications in determination of potential fields, *Manuscr. Geod.*, *20*, 8–20.

J. Kusche and E. J. O. Schrama, DEOS, Delft University of Technology, Kluyverweg 1, P.O. Box 5058, NL-2600 GB Delft, Netherlands. (j.kusche@lr.tudelft.nl; e.j.o.schrama@lr.tudelft.nl)

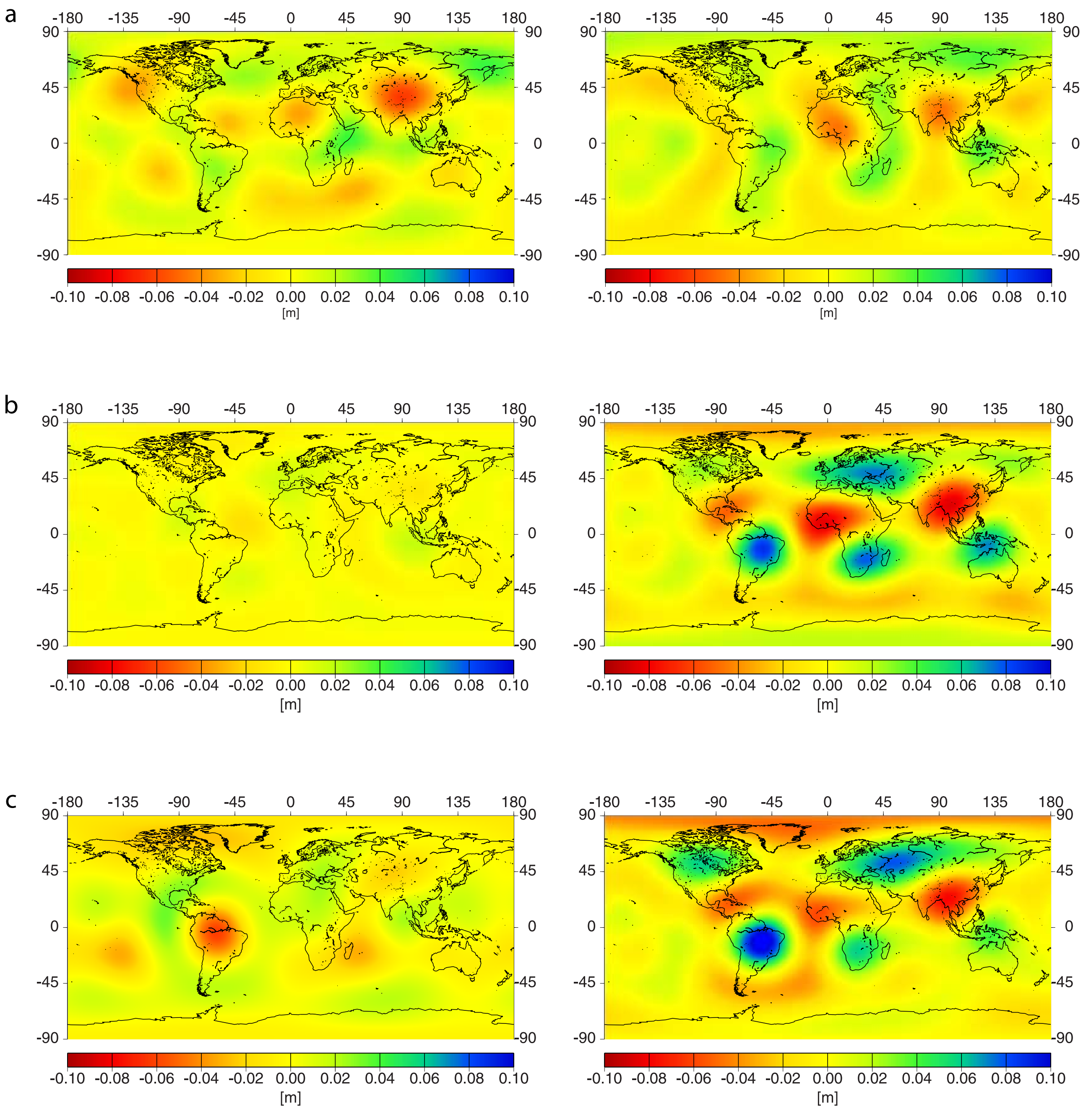

Figure 4. Annual surface density variation in equivalent water height [m], (a) from GPS inversion, $l = 3\ldots6$ (atmospheric effect removed (from NCEP)), (b) from CPC land hydrology model, $l = 3\ldots6$, and (c) from CSR GRACE models, $l = 3\ldots6$. (left) Cosine mode, (right) sine mode.